Available online at www.sciencedirect.com
SCIENCE DIRECT®
ELSEVIER
Applied Mathematical Modelling 29 (2005) 711–725
APPLIED MATHEMATICAL MODELLING
www.elsevier.com/locate/apm

An assessment of streamline curvature effects on the mixing region of a turbulent plane jet in crossflow

Manabendra Pathak, Anupam Dewan *, Anoop K. Dass

Department of Mechanical Engineering, Indian Institute of Technology Guwahati, Guwahati 781039, India

Received 1 March 2004; received in revised form 1 September 2004; accepted 13 October 2004
Available online 18 December 2004

Abstract

The flow field of a turbulent plane jet in a weak or moderate crossflow, which is characterised by mild streamline curvature, has been investigated computationally. The values of the jet-to-crossflow velocity ratios chosen are 6, 9 and 10. The time-averaged Navier–Stokes equations are solved on a staggered Cartesian grid using the standard k–ϵ model and the k–ϵ model with streamline curvature modification. The predictions using both the models are compared with available experimental data. It has been shown that by accounting for the effect of streamline curvature in the k–ϵ model results in good prediction of this flow configuration.
© 2004 Elsevier Inc. All rights reserved.

Keywords: Turbulence; Plane jet; Crossflow; Streamline curvature

1. Introduction

The study of turbulent jets in crossflow is important both from a practical point of view (e.g. jets used in V-STOL aircraft, film cooling of turbine blade, flow of exhaust gases in chimney stakes, discharge of sewage or waste into river or ocean) and from the basic research point of view, because of a variety of fluid dynamics phenomenon involved.

* Corresponding author. Present address: Institute of Fluid Mechanics (LSTM), Friedrich-Alexander University of Erlangen-Nuremburg, Cauerstr. 4, D-91058 Erlangen, Germany. Tel.: +49 9131 852 9477; fax: +49 9131 852 9503.
E-mail address: anupam.dewan@lstm.uni-erlangen.de (A. Dewan).

0307-904X/$ - see front matter © 2004 Elsevier Inc. All rights reserved.
doi:10.1016/j.apm.2004.10.010

Nomenclature

C_1	constant
C_2	constant
c	model constant
D	nozzle width at the exit
k	turbulent kinetic energy
n	coordinate perpendicular to jet trajectory
p	mean pressure
P_k	production of turbulent kinetic energy
R	jet to cross-stream velocity ratio (u_j/v_a)
R_f	flux Richardson number
s	distance along the jet trajectory from the center of jet slot
u	mean velocity along the jet discharge direction (x-direction)
U_e	s component of mean edge velocity
U_m	local maximum of the mean velocity
u'	fluctuating velocity component in x-direction
v	mean velocity along cross-stream direction (y-direction)
v'	fluctuating velocity component in y-direction
x	coordinate along the direction of the jet discharge
y	coordinate along the cross-stream direction
ϵ	rate of dissipation of turbulent kinetic energy k
v_t	eddy viscosity
ρ	density
σ_ϵ	model constant
σ_k	model constant
ϕ	model constant

Subscripts

a	ambient condition
j	jet condition at the discharge
max	maximum value

The flow field of turbulent jet in crossflow is basically three-dimensional. Owing to the presence of large coherent structures, strong pressure gradient across the jet, and the effects of side wall the flow becomes complex and three-dimensional. However in certain regions of the flow field the three-dimensional effects may not be significant. From the measurements of stream-wise velocity at several span-wise locations of a turbulent plane jet in weak and moderate crossflow, Ramaprian and Haniu [1,2] observed that the two-dimensionality of the velocity field is maintained within 12% of the jet slot around the central span-wise region. They measured less than 5% variation of velocity in the flow field ranging from the jet slot up to forty times of the jet slot distance in the downstream direction. However, further downstream the flow tends to loose its

two-dimensionality due to the side wall effects. Chen and Hwang [3] also observed that the temperature and velocity fields exhibit good two-dimensionality in the span-wise direction away from the side walls. Thus under such conditions a study of the two-dimensional flow field can represent sufficient characteristics of the flow field. Moreover as stated by Hahn and Choi [4], it is reasonable to explore the effect of some parameters on the computed field by investigating a rather simple and less time consuming situation, such as a two-dimensional flow field. Due its wide range of applications, the present flow configuration has been extensively investigated by many researchers. Acharya et al. [5] have provided a comprehensive review on the literature on film cooling. The flow behaviour and heat transfer analysis of jet in crossflow are found also in Carter [6], Sarkar and Bose [7], Hwang and Chiang [8] and Shi et al. [9]. In the present work only the flow behaviour of a plane jet in crossflow has been investigated. Some relevant works on the present flow configuration are found in Ramaprian and Haniu [1,2], Flacks et al. [10], McGurik and Rodi [11], Mikhail et al. [12], Hoda and Acharya [13], Keimasi et al. [14], and Kalita et al. [15].

The flow field of turbulent jet in crossflow is affected by several factors, such as velocity ratio of the jet and crossflow (R), injection angle, exit geometry, Reynolds numbers, jet spacing in case of multiple jets, etc. Demuren [16] classified the whole flow field into three zones, the potential core zone, the zone of maximum deflection and the far field zone. The potential core zone is the central part of the jet which spans from the jet source to few times of jet slot lengths. This zone is unaffected by the crossflow though its length is small in comparison to the jet in stagnant surroundings [16]. In the far field zone, the jet axis approaches the crossflow direction asymptotically and the flow field is nearly self similar. It is the second intermediate region, where the jet experiences maximum deflection. This region is complex, being characterised by mixing and interaction of both jet and crossflow on one side and streamline curvature on other.

The effect of streamline curvature on turbulence is a well established phenomenon and numerous literature (Bradshaw [17], Moser et al. [18], Holloway et al. [19]) are available describing the effect of streamline curvature on turbulence for the wall bounded flows. Experimental studies reviewed in Bradshaw [17] show that the magnitude of the turbulent shear stress and the degree of anisotropy between the normal stresses are sensitive to the streamline curvature. Curvature strongly influences the production as well as transport in shear layers. Due to the streamline curvature, there evolves an extra rate of strain in the flow field besides the main strain rate. Another important aspect of the flow field, which may have significant effect in the turbulence, is the presence of moving stream external to the jet. For numerical predictions of such complex flow field, either DNS, LES or full Reynolds stress transport model and anisotropy-resolving non-linear eddy-viscosity model can give a satisfactory performance. However being relatively simpler and computationally more efficient, two equation models (k–ϵ, k–ω) have been extensively used for the prediction of such flow fields with varying degrees of success (Sarkar and Bose [7], Hoda and Acharya [13], Keimasi et al. [14] and Kalita et al. [15]). Kalita et al. [15] used the standard k–ϵ model to investigate the experimental work of Ramaprian and Haniu [1,2] and reported a moderate success and this motivated the present work, where an effort is made to improve the numerical predictions of the flow field by considering the streamline curvature effect.

Numerous models have been proposed in the literature to account for the effect of streamline curvature on turbulent flow field in the formulation of the standard k–ϵ model. The streamline

curvature modification to the k–ϵ model, originally proposed by Leschziner and Rodi [20], for axi-symmetrical flow configuration was used by Kassimatis et al. [21] to investigate the aerodynamics of the near-slot film cooling. Kassimatis et al. [21] reported a slight improvement in the predictions in the recirculation region of the flow. Since the geometry of the present work is Cartesian and the flow field of the jet in crossflow is characterised by local curvature effect, the streamline curvature modification to the standard k–ϵ model proposed by Cheng and Farokhi [22] has been used. In this modification, algebraic formulation of eddy viscosity μ_t is done by extracting the extra strain rate and the main strain rate for the flow field with streamline curvature. This correction leads to a significant reduction in eddy viscosity around the separation streamline, i.e. in the curved shear layer bordering the recirculation. Moreover the model is more simple and computationally efficient than the Reynolds stress transport model or non-linear eddy-viscosity model. Cheng and Farokhi [22] used the model to study the backward-facing step flow and observed significant improvement in the results compared to the standard k–ϵ model. In the present work both the standard k–ϵ model and streamline curvature modification to k–ϵ model proposed by Cheng and Farokhi [20] are employed to predict the flow field of plane jet for the values of $R = 6$, 9 and 10 and the predictions are compared with the experimental findings of Ramaprian and Haniu [1,2].

2. Mathematical formulation

2.1. Governing equations

The flow configuration and the associated coordinates are shown in Fig. 1. We have considered a two-dimensional flow field where the jet is discharged normally with a uniform velocity of u_j through a slot of width D into a uniform cross-stream of velocity v_a. The flow is assumed to be incompressible and the molecular viscosity is neglected except in the near wall region. The Reynolds-averaged governing equations can be written as

(i) Continuity

$$\frac{\partial u}{\partial x}+\frac{\partial v}{\partial y}=0. \tag{1}$$

(ii) x-momentum

$$u\frac{\partial u}{\partial x}+v\frac{\partial u}{\partial y}=-\frac{1}{\rho}\frac{\partial p}{\partial x}+\frac{\partial}{\partial x}(-\overline{u'^2})+\frac{\partial}{\partial y}(-\overline{u'v'}). \tag{2}$$

(iii) y-momentum

$$u\frac{\partial v}{\partial x}+v\frac{\partial v}{\partial y}=-\frac{1}{\rho}\frac{\partial p}{\partial y}+\frac{\partial}{\partial x}(-\overline{u'v'})+\frac{\partial}{\partial y}(-\overline{v'^2}). \tag{3}$$

Here u and v are the mean velocities along the directions of the jet discharge (x-direction) and crossflow (y-direction), respectively and p is the mean pressure. The primed quantities represent fluctuations.

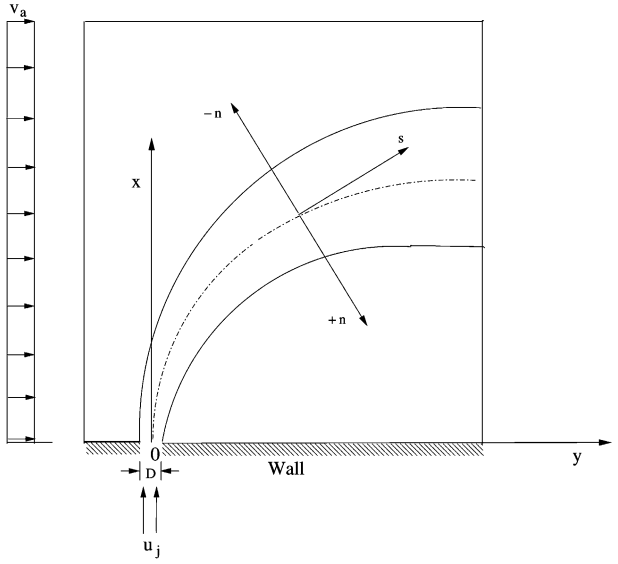


Fig. 1. Schematic diagram of the flow field.

2.2. Turbulence model

In the standard version of the k–ϵ model, the turbulent stresses are modeled as

$$-\overline{u'v'} = v_t\left(\frac{\partial u}{\partial y}+\frac{\partial v}{\partial x}\right), \tag{4}$$

$$-\overline{u'^2} = 2v_t\left(\frac{\partial u}{\partial x}\right)-\frac{2}{3}k, \tag{5}$$

$$-\overline{v'^2} = 2v_t\left(\frac{\partial v}{\partial y}\right)-\frac{2}{3}k, \tag{6}$$

where

$$v_t = c_\mu\frac{k^2}{\epsilon}. \tag{7}$$

Here v_t is the eddy viscosity, c_μ is a model constant, k is the turbulent kinetic energy and ϵ is the dissipation rate of turbulent kinetic energy. Both turbulent kinetic energy and dissipation are calculated from the following transport equations:

$$u\frac{\partial k}{\partial x}+v\frac{\partial k}{\partial y}=\frac{\partial}{\partial x}\left(\frac{v_t}{\sigma_k}\frac{\partial k}{\partial x}\right)+\frac{\partial}{\partial y}\left(\frac{v_t}{\sigma_k}\frac{\partial k}{\partial y}\right)+P_k-\epsilon, \tag{8}$$

$$u\frac{\partial \epsilon}{\partial x}+v\frac{\partial \epsilon}{\partial y}=\frac{\partial}{\partial x}\left(\frac{v_t}{\sigma_\epsilon}\frac{\partial \epsilon}{\partial x}\right)+\frac{\partial}{\partial y}\left(\frac{v_t}{\sigma_\epsilon}\frac{\partial \epsilon}{\partial y}\right)+c_1\frac{\epsilon}{k}P_{\mathrm{k}}-c_2\frac{\epsilon^2}{k}, \tag{9}$$

where P_{k} is the rate of production of k and is given by

$$P_{\mathrm{k}}=v_t\left[\left(\frac{\partial u}{\partial y}+\frac{\partial v}{\partial x}\right)^2+2\left(\frac{\partial u}{\partial x}\right)^2+2\left(\frac{\partial v}{\partial y}\right)^2\right]. \tag{10}$$

The values of the model constants used in the above equations are $c_\mu=0.09$, $c_1=1.44$, $c_2=1.92$, $\sigma_{\mathrm{k}}=1.0$, $\sigma_\epsilon=1.3$ [23].

2.3. Curvature modification model

Cheng and Farokhi [22] derived the streamline curvature modification to the standard k–ϵ model from the algebraic Reynolds stress model proposed by Rodi [24]. In this modification, v_t is given as

$$v_t=\frac{k^2}{\epsilon}\frac{2\phi}{3}\left[1-R_{\mathrm{f}}-\phi\frac{P_{\mathrm{k}}}{\epsilon}\frac{R_{\mathrm{f}}^2+4R_{\mathrm{f}}+1}{1-R_{\mathrm{f}}}\right]. \tag{11}$$

Here ϕ is a model constant given by

$$\phi=\frac{1-C_2}{C_1-1+\dfrac{P_{\mathrm{k}}}{\epsilon}}$$

and $C_1=1.5$ and $C_2=0.76$ are the inertial and forced return-to-isotropy constants respectively. R_{f} is the flux Richardson number given by

$$R_{\mathrm{f}}=-\frac{\partial v/\partial x}{\partial u/\partial y}. \tag{12}$$

The form of flux Richardson number used in this work was used by Cheng and Farokhi [22] for predicting the backward facing step flow, where the flow is predominant in the x-direction and is characterised by weak curvature. The present work is also characterised by weak curvature and the flow is predominant along the x-direction (the jet discharge direction) in the mixing region. Hence though the flux Richardson number is not frame invariant, its application to the present flow configuration is justified as its implementation is simple and consistent with the physical nature of the flow. The flux Richardson number R_{f} plays an important role as it dictates the effect of streamline curvature on the turbulence structure through the amplification and diminution of the eddy viscosity.

It easily follows from Eqs. (7) and (11) that

$$c_\mu=\frac{2\phi}{3}\left[1-R_{\mathrm{f}}-\phi\frac{P_{\mathrm{k}}}{\epsilon}\frac{R_{\mathrm{f}}^2+4R_{\mathrm{f}}+1}{1-R_{\mathrm{f}}}\right]. \tag{13}$$

When local streamline curvature effect vanishes $R_{\mathrm{f}}=0$ and the value of c_μ becomes equal to the standard value of 0.09 and the model reduces to the standard k–ϵ model.

3. Computational methodology

The governing equations involved in this problem are elliptic in nature. A computer code has been developed to solve the equations using the SIMPLER algorithm [25]. The code employs a non-uniform staggered grid in which the velocity components are positioned on the control volume surfaces and scalar variables (p, k and ϵ) are positioned at the center of each control volume. The convection and diffusion terms of the governing equations are discretised using the power-law scheme [25]. The ADI (alternating the direction of line-by-line iteration) scheme using the tri-diagonal matrix algorithm is used to solve the system of linear algebraic equations. All the variables (u, v, k, and ϵ) are under-relaxed at each iteration.

The present code is validated by comparing the predicted centerline mean velocity decay with the results of Seyedein et al. [26], who numerically studied the turbulent confined slot jet impingement using the standard k–ϵ model. The agreement is found to be good with a difference of less than 4% at any location of the flow field.

4. Computational domain and grid size

The computational domain (Fig. 1) for the present work is rectangular. The left boundary from which the cross-stream enters the domain is positioned sufficiently far away up-stream from the jet discharge slot as suggested by Amer et al. [27] and the right boundary is placed sufficiently away downstream from the jet source, such that the zero gradient condition for all the variables can be applied there [28]. The bottom boundary is the wall from which the jet emanates and the top boundary is placed sufficiently away from the bottom so that the cross-stream velocity condition can be applied there [8]. In the crossflow direction, the computational domain extends from $10D$ (D is the width of the slot) upstream of the center of the jet to $168D$ downstream. The separation between the top and bottom boundaries depends upon the value of R and is selected in such a way so that the aforementioned boundary conditions can be applied. For example, for $R = 6$ a separation of $240D$ is considered.

The grid independent test of the computation is checked with four different sets of grids, viz. 60×40 (60 along x- and 40 along y-directions), 70×50, 80×60 and 90×70 by comparing a sensitive parameter turbulent kinetic energy for each case. The grids are non-uniform in both directions and clustered near the wall and the jet source region. The profile of the turbulent kinetic energy for $R = 6$ at $y/D = 25.0$ using the standard k–ϵ model is shown in Fig. 2. It has been observed that the grid refinement in general improves the near field solution without significantly altering the far field solution. The deviation between the predictions using four different grids decreases as the mesh is refined and the difference between the predictions using the grid sizes 80×60 and 90×70 is small. The results that are presented in the subsequent sections are for the grid size 80×60.

5. Boundary conditions

The different boundary conditions used in the present computations are inlet, outlet and wall. The whole bottom boundary excluding the jet discharge, is considered as a solid wall where the

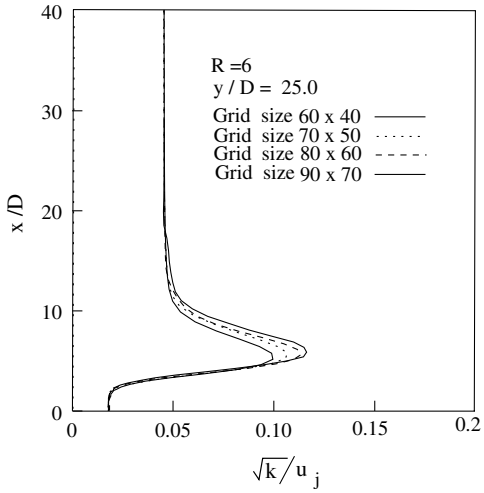


Fig. 2. Grid sensitivity test.

boundary conditions are applied using the standard wall functions [23]. The universal logarithmic velocity profile is assumed to prevail in the vicinity of the bottom wall. Turbulent kinetic energy is set to be zero at the bottom wall, and its dissipation rate in the near wall region is assumed to be inversely proportional to the distance from the wall [29]. The boundary conditions at the left boundary are the free stream conditions, i.e, $u = 0$, $v = v_a$, $k = 0.04v_a^2$ and $\epsilon = k^{3/2}/0.06x_{max}$. The same free stream conditions are applied at the top boundary. At the right boundary, normal gradient of all variables are considered to be zero. The jet inlet velocity profile used in this work is a uniform velocity profile as used in the experimental work of Ramaprian and Haniu [1,2]. At the jet discharge region, the boundary conditions are $u = u_j$, $v = 0$, $k_j = 0.001u_j^2$ and $\epsilon = k^{3/2}/0.5D$. Since the velocities at the boundaries are specified, there is no need of specifications of pressure at the boundaries [25] and hence no boundary values for the pressure are prescribed.

6. Results and discussion

The present computational results of the mean velocity components and turbulent shear stresses of turbulent plane jet in crossflow are compared with the experimental observations made by Ramaprian and Haniu [1,2]. Ramaprian and Haniu [1,2] have reported their experimental observations in the *s–n* coordinate system (see Fig. 1). They reported their experimental uncertainties in the mean velocity as 8% and in turbulent stress as 10% [1]. The flow configuration of a two-dimensional turbulent plane jet in crossflow configuration can be analysed either from the point of view that the jet is deflected due to the momentum of crossflow or the jet completely obstructs the crossflow. The upper part of the deflected jet ($n/D < 0$) faces and mixes with the crossflow. This part of the jet is referred to as the outer portion and the other part of the jet ($n/D > 0$) is referred to as the inner portion of the jet.

The jet trajectory is one important parameter to be analysed for a jet in a crossflow. It is defined as the locus of the local maximum velocity and it presents qualitative representation of the flow

and the jet deflection. In Fig. 3, predicted jet trajectories are compared with the experimental data for $R = 6$, 9 and 10. Since the crossflow is relatively weak, the jet is almost unaffected by the crossflow in the vicinity of discharge, but further downstream as s increases, the jet gets increasingly deflected due to a larger momentum of the crossflow. Both turbulence models compare well with the experimental data. It is also observed that higher the value of R, higher is the depth of penetration of the jet and smaller is its deflection. Therefore the jet with the value of $R = 6$ experiences higher deflection and thus the effect of streamline curvature will be higher in this case compared to the cases with $R = 9$ and 10.

The local maximum mean velocity (U_m) of the jet decreases along the jet trajectory due to the mixing of the jet with crossflow. The normalised maximum velocity decay is shown in Fig. 4. The prediction of the decay rate using the streamline curvature modification to the k–ϵ model are better compared to the predictions using the standard k–ϵ model. This is due to the counter effect imparted by the cross-velocity at the edge of the jet, which is captured by the streamline curvature modification model and not by the standard k–ϵ model.

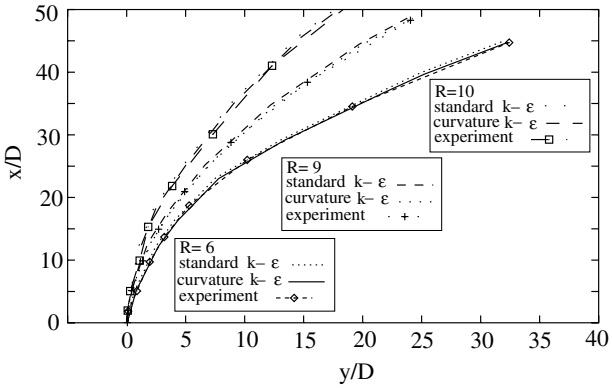


Fig. 3. Comparison of jet trajectory for $R = 6$, 9 and 10 with experimental data (Fig. 2 [2]).

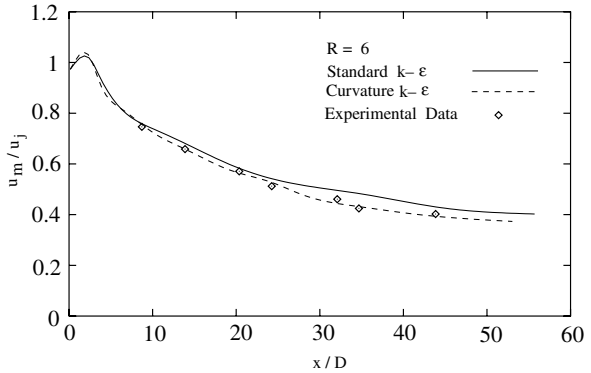


Fig. 4. Comparison of decay of maximum velocity for $R = 6$ (experimental data Fig. 3.22 [1]).

The normalised s-component profiles of the mean velocity u are shown in Figs. 5 and 6 for values of $R = 6$ and 9 respectively, at different s/D locations. It is observed that the jet spreads with distance along the stream-wise direction. It is also observed that jet tends to become symmetric as the distance from the jet source increases due to the absence of strong crossflow or decay of cross-velocity. The curvature modification model should show the enhanced spreading rate in the outer part ($n/D < 0$) and reduced spreading rate in the inner part ($n/D > 0$) of the jet. However due to the moving stream of the crossflow the effects of curvature and co-flowing ambient counteract each other. Hence the spreading rate is depressed in the outer portion of the jet. The improvement of the curvature modification is seen in the inner part of the jet by observing the reduction of spreading rate and more prominently at the edge of the inner portion by showing negative velocity (for the location $s/D = 9.68$, 18.86 and 21.22), thereby accurately predicting mild recirculation below the jet. It is also observed that the improvement in the prediction by the curvature modification to k–ϵ model compared to the standard k–ϵ model is small for the case of jet with $R = 9$, because the flow experiences small streamline curvature.

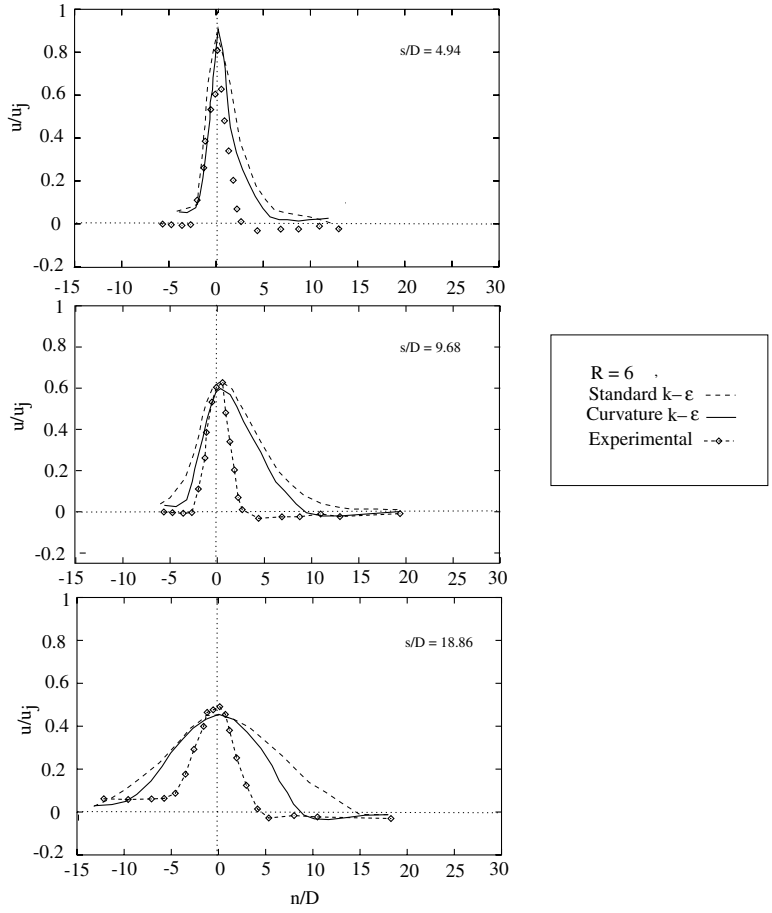


Fig. 5. Comparison of predicted u/u_j profiles for $R = 6$ (experimental data run no. 12015, 12016 and 12018, respectively, [1]).

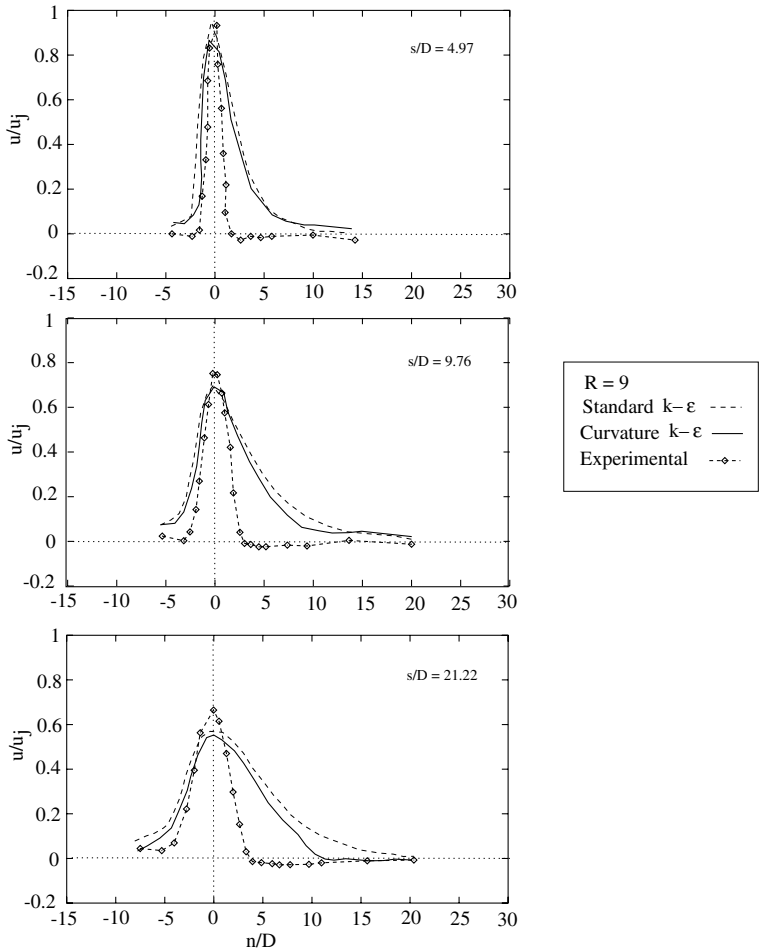


Fig. 6. Comparison of predicted u/u_j profiles for $R = 9$ (experimental data run no. 12057, 12058 and 12053, respectively, [1]).

The normalised n-component profiles of the mean velocity v are shown in Figs. 7 and 8 for values of $R = 6$ and 9, respectively, at different s/D locations. Here also due to the effect of finite edge velocity the spreading rate is reduced in the outer part of the jet. Moreover the streamline curvature modification shows better performance in the case of $R = 6$ than in the case of $R = 9$.

The normalised turbulent shear stresses are shown in Figs. 9 and 10 respectively for the jet $R = 6$ and 9. It is found from the literature [30] that the value of maximum normalized shear stress for turbulent jet in a quiescent ambience is 0.022. Compared to this value, there should be an enhancement of the shear stress in the outer portion and a reduction in the inner portion of the jet due to streamline curvature in the present case. Due to the combined effect of streamline curvature and edge velocity, the streamline curvature modification model does not show adequate increase of shear stress in the outer part of the jet, but it shows an appreciable reduction of the shear stress in the inner region compared to that predicted by the standard k–ϵ model. The standard k–ϵ model

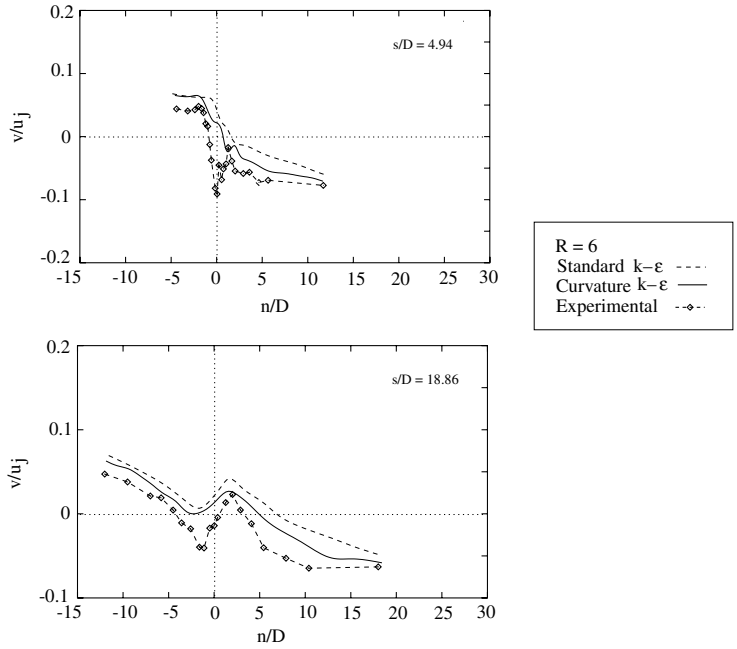


Fig. 7. Comparison of predicted v/u_j profiles for $R = 6$ (experimental data run no. 12015 and 12018 [1]).

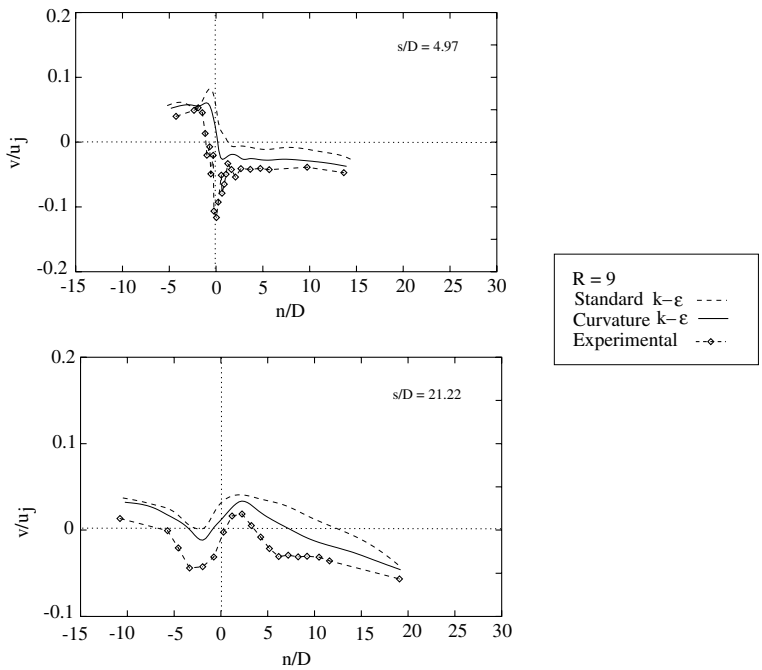


Fig. 8. Comparison of predicted v/u_j profiles for $R = 9$ (experimental data run no. 12057 and 12053 [1]).

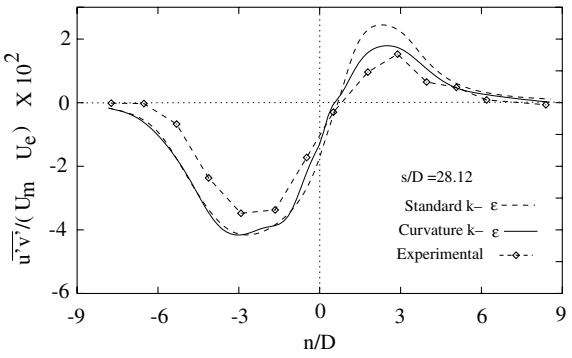


Fig. 9. Comparison of turbulent shear stress profiles for $R = 6$ (experimental data Fig. 4.7 [1]).

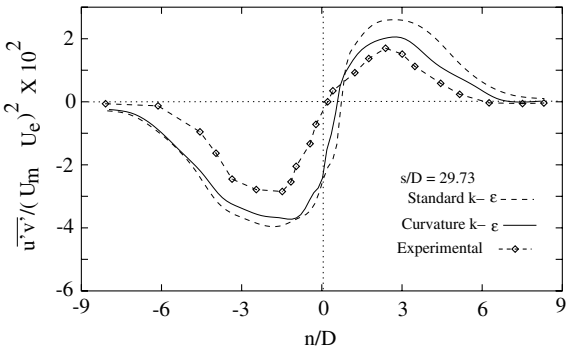


Fig. 10. Comparison of turbulent shear stress profiles for $R = 9$ (experimental data Fig. 4.6 [1]).

over predicts the shear stress in the inner part of the jet. It is also observed that the location of zero shear stress predicted by the two models does not coincide with the center of the jet.

7. Conclusions

The flow field of a two-dimensional turbulent plane jet in a weak crossflow is numerically investigated by employing the effect of streamline curvature in the mean and turbulent flow properties. The important predicted flow properties such as jet trajectory, velocity decay, mean flow profiles and turbulent stresses have been compared with the experimental data. The predictions by the streamline curvature modification to the k–ϵ model have been shown to be in good agreement with the experimental data.

Acknowledgement

Anupam Dewan acknowledges the support provided by the Department of Science and Technology, Government of India, New Delhi, under the Fast Track sponsored project no. HR/OY/E-05/99 (SR/FTP/E-05/99).

References

[1] B.R. Ramaprian, H. Haniu, Turbulence measurement in plane jets and plumes in cross flow. Technical Report No. 266, IIHR, University of Iowa, Iowa City, IA, 1983.
[2] H. Haniu, B.R. Ramaprian, Studies on two-dimensional curved nonbuoyant jets in cross flow, ASME J. Fluid Eng. 111 (1989) 78–86.
[3] K.S. Chen, J.Y. Hwang, Experimental study on the mixing of one and dual-line heated jets with a cold crossflow in a confined channel, AIAA J. 29 (3) (1991) 353–360.
[4] S. Hahn, H. Choi, Unsteady Simulation of jets in a cross flow, J. Comput. Phys. 134 (1997) 342–356.
[5] S. Acharya, M. Tyagi, A. Hoda, Flow and heat transfer predictions for film cooling, heat transfer in gas turbine systems, Ann. N.Y. Acad. Sci. 934 (2001) 110–125.
[6] H.H. Carter, A preliminary report on the characteristics of a heated jet discharged horizontally into a transverse current, Part 1-Constant depth, Technical Report No. 61, Chesapeake Bay Inst., Johns Hopkins University, Baltimore, MD, 1969.
[7] S. Sarkar, T.K. Bose, Comparison of different turbulence models for prediction of slot-film cooling: flow and temperature field, Numer. Heat Transfer, Part B 28 (1995) 217–238.
[8] R.R. Hwang, T.P. Chiang, Numerical simulation vertical forced plume in a crossflow of stably stratified fluid, ASME J. Fluid Eng. 117 (1995) 696–705.
[9] Y. Shi, M.B. Ray, A.S. Mujumdar, Numerical study on the effect of cross-flow on turbulent flow and heat transfer characteristics under normal and oblique semi-confined impinging slots jets, Drying Technol. 21 (10) (2003) 1923–1939.
[10] R. Flacks, K. Dullenkopf, V. Scherer, Constituency measurements in the mixing region of a cross flow jet using a laser velocimeter, Exp. Fluids 17 (1994) 198–204.
[11] J.J. McGurik, W. Rodi, A depth-averaged mathematical model for the near field of side discharges into open-channel flow, J. Fluid Mech. 86 (1978) 761–781.
[12] R. Mikhail, V.H. Chu, S.B. Savage, The reattachment of a two-dimensional turbulent jet in a confined cross flow. In: Proc. 16th IAHR Cong. 3, Sao Paulo, Brazil, 1975, pp. 414–419.
[13] A. Hoda, S. Acharya, Predictions of a film coolant jet in crossflow with different turbulence models, ASME J. Turbomachinery 122 (2000) 558–569.
[14] R. Keimasi, T. Rahni, Numerical simulation of jets in a crossflow using different turbulence models, AIAA J. 39 (12) (2001) 2268–2277.
[15] K. Kalita, A. Dewan, A.K. Dass, Prediction of turbulent plane jet in crossflow, Numer. Heat Transfer, Part A 41 (2002) 1–12.
[16] A.O. Demuren, Modeling turbulent jets in crossflow, in: N.P. Cheremisinoff (Ed.), Encyclopedia of Fluid Mechanics, vol. 2, Gulf Publishing Company, Houston, TX, 1986, [Chapter 17].
[17] P. Bradshaw, The effects of streamline curvature on turbulent flow, AGARDograph no. 169, 1969.
[18] D. Moser, D. Robert, P. Moin, The effects of curvature in wall-bounded turbulent flows, J. Fluid Mech. 175 (1986) 479–510.
[19] A.G.L. Holloway, S. Tavoularis, The effects of curvature on sheared turbulence, J. Fluid Mech. 237 (1992) 569–603.
[20] M.A. Leschzine, W. Rodi, Calculation of annular and twin parallel jets using various descretization schemes and turbulence-model variations, ASME J. Fluid Eng. 103 (1981) 352–360.
[21] P.G. Kassimatis, G.C. Bergeles, T.V. Jones, J.W. Chew, Numerical investigation of the aerodynamics of the near-slot film cooling, Int. J. Numer. Methods Fluids 32 (2000) 97–117.
[22] G.C. Cheng, S. Farokhi, On turbulent flows dominated by curvature effects, ASME J. Fluid Eng. 114 (1992) 52–57.
[23] B.E. Launder, D.B. Spalding, The numerical prediction of turbulent flow, Comput. Methods Appl. Mech. Eng. 3 (1974) 269–289.
[24] W. Rodi, A new algebraic relation for calculating the Reynolds stresses, Z. Angew. Math. Mech. 56 (1976) T219–T221.
[25] S.V. Patankar, Numerical Heat Transfer and Fluid Flow, Hemisphere Publishing Corporation, New York, 1980.

[26] S.H. Seyedein, M. Hasan, A.S. Mujumdar, Modelling of a single confined turbulent slot jet impingement using various k–ϵ turbulence models, Appl. Math. Modell. 18 (1994) 526–537.
[27] A.A. Amer, B.A. Jubran, M.A. Hamdan, Comparison of different two-equation turbulence models for prediction of film cooling from two rows of holes, Numer. Heat Transfer, Part A 21 (1992) 143–162.
[28] R.I. Sykes, W.S. Lewellen, S.F. Parker, On the vorticity dynamics of turbulent jet in crossflow, J. Fluid Mech. 168 (1986) 393–413.
[29] S.V. Patankar, D.K. Basu, S.A. Alpay, Prediction of three-dimensional velocity field of a deflected tirbulent jet, ASME J. Fluid Eng. 99 (1977) 758–762.
[30] B.R. Ramaprian, M.S. Chandrasekhara, LDA measurements in plane turbulent jets, ASME J. Fluid Eng. 107 (1985) 264–271.